IRRADIATION OF INERT MATRIX AND MIXED OXIDE FUEL IN THE HALDEN TEST REACTOR

Ch. Hellwig, U. Kasemeyer

In a new type of fuel, called Inert Matrix Fuel (IMF), plutonium is embedded in a U-free matrix. This offers advantages for more efficient plutonium consumption, higher proliferation resistance, and for inert behaviour later in a waste repository. In the fuel type investigated at PSI, plutonium is dissolved in yttrium-stabilised zirconium oxide (YSZ), a highly radiation-resistant cubic phase, with addition of erbium as burnable poison for reactivity control. A first irradiation experiment of YSZ-based IMF is ongoing in the OECD Material Test Reactor in Halden (HBWR), together with MOX fuel (Rig IFA-651.1). The experiment is described herein and results are presented of the first 120 days of irradiation with an average assembly burnup of 47 kWd/cm^3. The results are compared with neutronic calculations performed before the experiment, and are used to model the fuel behaviour with the PSI-modified TRANSURANUS code. The measured fuel temperatures are within the expected range. An unexpectedly strong densification of the IMF during the first irradiation cycle does not alter the fuel temperatures. An explanation for this behaviour is proposed. The irradiation at higher linear heat rates during forthcoming cycles will deliver information about the fission gas release behaviour of the IMF.

1 INTRODUCTION

In a new type of fuel, called Inert Matrix Fuel (IMF), plutonium is embedded in a U-free matrix. This allows the plutonium to be burned without generating fresh amounts by neutron capture in U^{238}, and thus to achieve a more efficient consumption of plutonium than for Mixed Oxide Fuel (MOX). The fuel research at PSI has latterly concentrated efforts in this field on a ZrO_2-based matrix. In this fuel, plutonium is dissolved in yttrium-stabilised zirconium oxide (YSZ), a highly radiation-resistant cubic phase with the potential of achieving high burnup [1]. The IMF is designed to replace MOX in conventional fuel assemblies. Erbium has to be added as burnable poison to the fuel for reasons of reactivity control [2].

Further advantages of the new fuel type result from the chosen matrix, which is not only neutronically, but also chemically, inert. The extreme insolubility of the matrix is of advantage with regard to cladding failure in the reactor, preventing the wash-out of fissile material and fission products. The spent fuel assemblies would be ready to be sent for direct waste disposal with only little conditioning, as the fission products are already embedded in an inert matrix [3]. The extreme difficulties in dissolving the matrix are also an important factor for non-proliferation reasons.

After years of basic research on the properties of this new fuel [4-9], a first irradiation experiment of YSZ-based IMF is ongoing in the OECD Material Test Reactor in Halden (HBWR), together with MOX fuel (Rig IFA-651.1) [10]. The present report gives an overview of the irradiation experiment in Halden, its layout, the results obtained to date, and the plans for further irradiation tests.

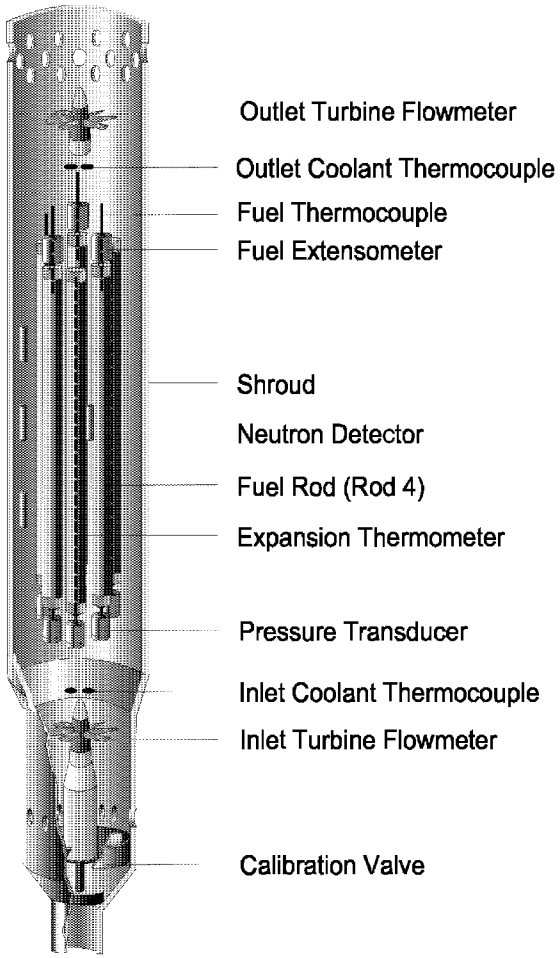

Fig. 1: Schematic of IFA-651.1 rig.

2 EXPERIMENTAL DETAILS

The irradiation experiment IFA-651.1, with IMF based on YSZ and MOX fuel, started as part of the OECD Halden Reactor Project at the end of June, 2000. The aim of this experiment was to measure the central line temperature, its change with burnup, fission gas release, densification and swelling, and the general thermal behaviour of these fuels. The first cycle was

completed after 120 days, and an average assembly burnup of 47 kWd/cm^3 (i.e. 4.5 MWd/kg$_{MOX}$ for MOX fuel) was achieved. Note that this unconventional unit for burnup (produced energy per unit volume) was chosen because IMF and MOX fuel have very different densities; the unit is frequently used in connection with IMF.

2.1 IFA-651.1

In IFA-651.1 (IFA = Instrumented Fuel Assembly), the rods are equipped with expansion thermometers (ETs), thermocouples (TFs), fuel extensometers (EFs), and pressure transducers (PFs). To position the TFs, a hole was drilled about 50 mm into the fuel stack. The TF was then inserted to a depth of about 38 mm. For the ETs, a central hole was drilled in the whole fuel column. Table 1 summarizes the instrumentation of the various fuel rods, and Fig. 1 shows a schematic of the IFA-651.1 rig. In order to obtain a good record of the axial power distribution, the assembly is instrumented with three axial Neutron Detectors (NDs). The radial power profile is determined by three radially arranged NDs, which are placed on the central axis of the assembly.

Table 1: Instrumentation and positions of the various fuel rods within IFA-651.1

Rig Position	**1**	**2**	**3**
Fuel Designation	MOX-SBR	IMF-ATT-1	MOX-ATT-1
Fabr. Method	SBR	Dry Mill	Dry Mill
Instrumentation	TF,PF	TF,PF,EF	ET,PF
Free Volume	25%	30%	30%
Rig Position	**4**	**5**	6
Fuel Designation	IMF-CO	IMF-ATT-2	MOX-ATT-2
Fabr. Method	Co-Prec	Dry Mill	Dry Mill
Instrumentation	TF,PF,EF	ET,PF	TF,PF,EF
Free Volume	30%	30%	30%

ET: Expansion Thermometer; TF: Thermocouple; PF: Pressure Transducer; EF: Fuel Extensometer

2.2 Power Determination

All parameters describing the fuel behaviour, such as fuel central temperature, pressure, stack elongation, are real-time and in-core measured values, while those relating to the power (linear heat rate, burnup) depend on neutron physics calculations. Such calculations were performed in preparation of the experiment using the two-dimensional transport code HELIOS [11], with its cross-section library based on ENDF/B-VI [12], to determine power, power distribution in the rig, depletion function, fission gas production rates, and the radial power distributions within the IMF and MOX fuel rods. Therefore, IFA-651.1 was modelled within an average environment of the Halden Reactor. Figure 2 shows IFA-651.1 in this environment. It was modelled as an infinite configuration with critical buckling, so that the neutron spectrum was the same as the average neutron spectrum in the Halden Boiling Water Reactor

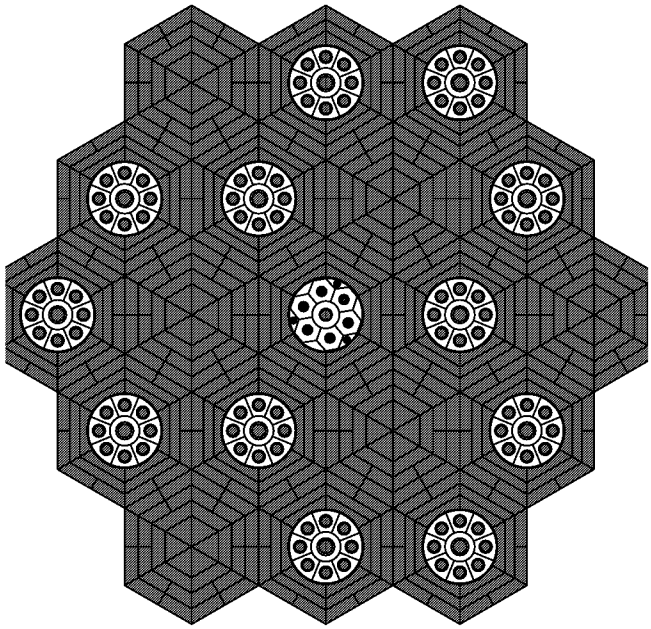

Fig. 2: The environment of IFA-651.1 in the Halden Boiling Water Reactor as it was used for the layout calculations with HELIOS.

(HBWR). The enrichment of the rods was chosen in such a way that all rods have similar power, and would achieve similar burnup.

During the measurement, the power of each rod is determined by multiplying a rod-dependent, power conversion factor (PCF) with the neutron detector signal, which measures the actual flux in the experiment, and a depletion function. Both PCF and the depletion function are calculated by HELIOS. The power conversion factor transforms the measured neutron detector signal into the rod power at beginning of cycle, while the depletion function describes the power reduction with burnup. Hence, the calculation of the PCFs can be validated through a power calibration at beginning of cycle, while the depletion function and burnup calculation can be validated by a second or third power calibration at certain burnup points.

During power calibration, the relation between the power production and the average ND-signal of the rig is measured. The power production is determined by measuring the (sub-cooled) water flow in the rig, and its temperature increase as a result of the heat production in the fuel rods. Subtracting the γ-heating from the measured power gives the rod power production. The relation of this power to the ND-signal is the so-called KG-factor, which can also be calculated by HELIOS.

Two power calibrations were carried out, one at beginning of cycle, and one at the end of cycle. In the first case, the KG-factor was measured to be 0.750 kW/nA, while the predicted value was 0.772 kW/nA. This means that the calculated value was 3% higher than the measured one, and was within the uncertainty range of the measurement. The second power calibration was carried out at an

average assembly burnup of 47.1 kWd/cm^3. The average depletion function of the assembly was measured to be 0.935, while the predicted value was 0.942, only 0.8% too high. This indicates that the neutron physics behaviour of such novel Inert-Matrix Fuel can be simulated quite accurately.

After the first power calibration, all PCFs were reduced by 3% to adjust the calculated values to the measured ones so that the power conversion factors continue to include the calculated rod power distribution; the depletion function cannot be adapted (it is a fourth order polynomial). The calculated function will then be used for the whole irradiation time.

Figure 3 shows the calculated radial power distributions of IMF in comparison to that of MOX fuel. In IMF, the relative power decreases at the rim and increases by 40 to 50% at the fuel centre as burnup increases from 0 to 440 kWd/cm^3; there is no build up of new plutonium from uranium in IMF. This effect must be taken into account during measurement in order to estimate the degradation of the thermal conductivity during burnup. For MOX fuel, the increase of relative power at the fuel centre is lower, and the typical rim effect arises.

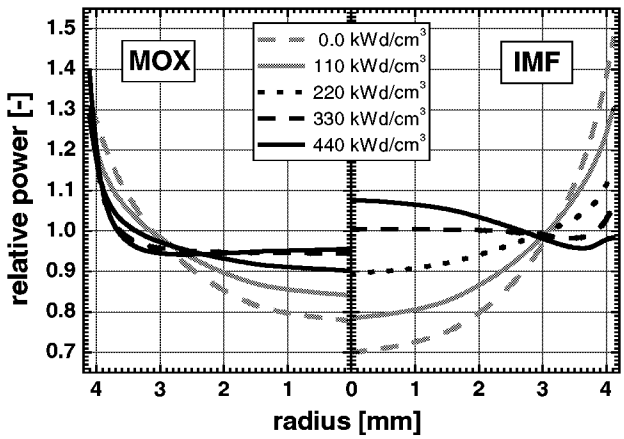

Fig. 3: Change of radial power distribution in IMF and MOX fuels as functions of burnup.

2.3 Fuel

The test contains three rods of IMF and three rods of MOX fuel. The IMF for two rods was fabricated by a dry attrition mill method (IMF-ATT), while the third IMF rod was fabricated by a wet process (IMF-CO).

For IMF-ATT, the powder constituents (ZrO_2, PuO_2, YO_2 and ErO_2) were mixed together in a vessel, stirred mechanically, and then milled to a homogeneous powder in the attrition mill. To increase the fluidity, the powder was precompacted with low pressure, and then broken again to granules in a granulator; 0.4wt% zinc stearate as lubricant was admixed to the granulated powder before compaction. The pellets were pressed at 500 MPa, and then sintered at 1450°C for 6h in a CO_2 atmosphere. The pellet density determined by water immersion was 95% of the theoretical density. The grain size was difficult to determine, but was of the order of 5 µm.

For IMF-CO, microspheres with the desired composition were produced by internal gelation, dried at 200°C, and calcined at 550°C in an argon atmosphere. The calcined spheres were crushed by an automatic mortar to particles, and then milled in the attrition mill to fine powder. Granulation and pelletizing of this material was carried out in the same way as for IMF-ATT. The green pellets were sintered at 1700°C for 6h in an N_2+8H_2 atmosphere. The pellet density determined by water immersion was 92% of the theoretical density for one batch, and 86% for a second batch. The grain size was of the order of 25 µm.

MOX-ATT fuel rods were produced in the same way as IMF-ATT (mixing PuO_2 and UO_2 powder before attrition milling) [13]. Sintering was performed at 1450°C in a CO_2 atmosphere for 5h, reaching a sintered density of the pellets of 95%, and a grain size of the order of 10 µm. Additionally, one, commercial fuel rod with short-binderless route (SBR) MOX fuel from BNFL was used as reference [14]. The Pu_{fiss} content was 0.54 g/cm^3 for MOX, 0.7 g/cm^3 for IMF-ATT, and 0.61, 0.65 g/cm^3 for the two IMF-CO batches, respectively.

2.4 Power History

The power history of the rig is typical for the HBWR (see Fig.4). Maximum power was achieved after 15.5 days, and reached between 26.3 kW/m (for rod 1) and 23.4 kW/m (for rod 3).

The achieved burnup after this first cycle in the HBWR was between 45.1 kWd/cm^3 (rod 4) and 49.6 kWd/cm^3 (rod 5).

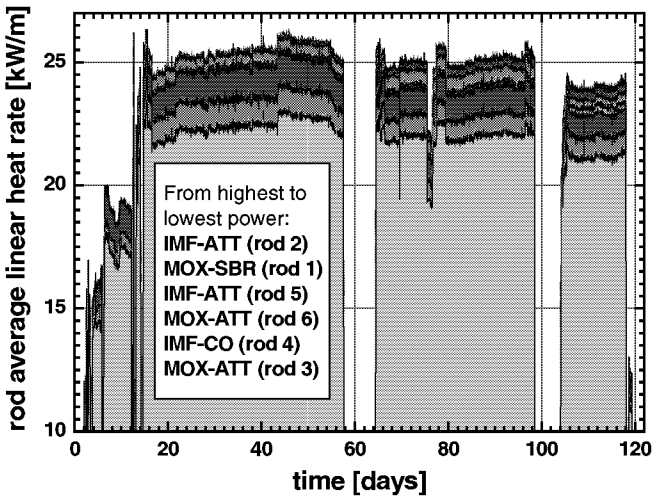

Fig 4: Average linear heat rate vs. time for IFA-651.1.

3 RESULTS

3.1 Fuel Behaviour

The measured centre temperatures for the fresh fuel are within the expected range for both IMF and MOX fuel. Figure 5 shows the measured temperatures. It is obvious that all IMF rods reached significantly higher temperatures due to their lower thermal conductivity compared with the MOX rods.

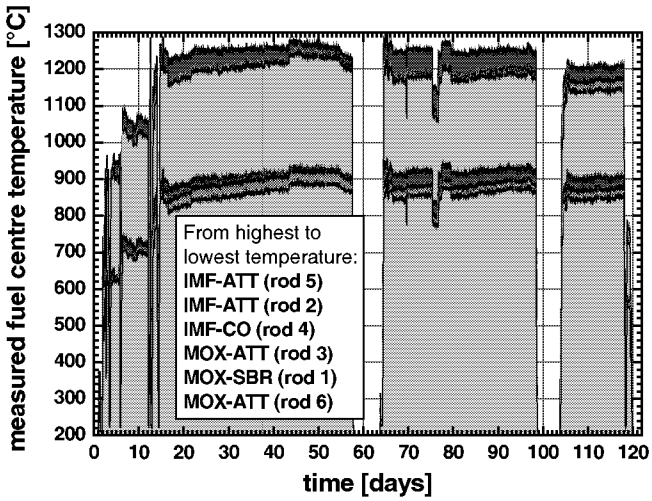

Fig. 5: Measured temperatures vs. time for IFA-651.1.

The pressure is decreasing in all six rods (see Fig. 6). This indicates densification of the fuel (i.e. increase in free rod volume), while fission gas release was not detected due to the low burnup. The densification could also be observed from the stack elongation measurement (see Fig. 7).

The densification of the PSI-MOX fuel is similarly low, and reaches approximately 1.0% (rod 3) and 1.7% (rod 6) after 15 kWd/cm^3 burnup (SBR-MOX, rod 1: 2.0%).

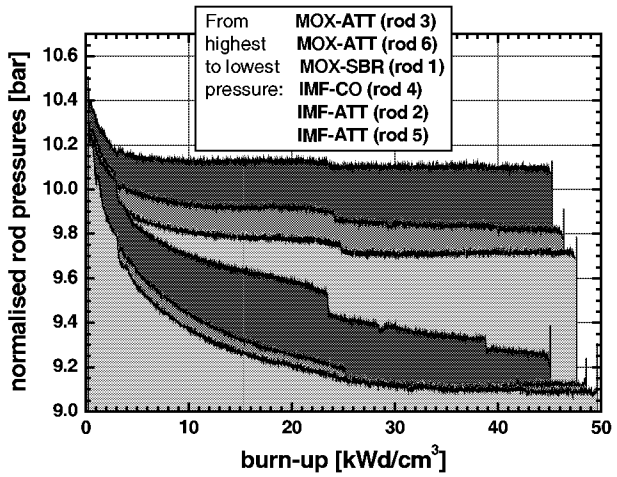

Fig. 6: Normalised pressure vs. burnup for IFA-651.1.

The densification found in IMF is unexpectedly high. Both IMF-ATT rods sinter to nearly 100% of the theoretical density within 35 kWd/cm^3 burnup. IMF-CO shows a slower densification than IMF-ATT: it is still in progress after 120 days and a burnup of 45 kWd/cm^3. This can be explained by the much smaller grain size in IMF-ATT, and thereby an enhanced ability to restructure.

In spite of the strong densification, the fuel temperatures of the IMF fuel also stayed stable. Figure 8 shows the fuel centre temperatures, normalised to a power of 25 kW/m, in a time range in which significant densification takes place (see Fig. 7). The two IMF rods show the same gradual increase in temperature compared with the three MOX rods, due to the densification and the resulting increase in gap width. One IMF rod with an elongation thermometer (rod 5), and therefore fuelled only with annular pellets, shows even a slight decrease of the normalised temperature.

In MOX fuel, the densification during irradiation is limited in the specifications in order to avoid the formation of a large gap, and consequently a large increase of the fuel temperatures. It is remarkable that the high and fast densification in IMF does not alter the fuel centre temperatures significantly. An explanation, and a model for this new behaviour, are proposed in the next section.

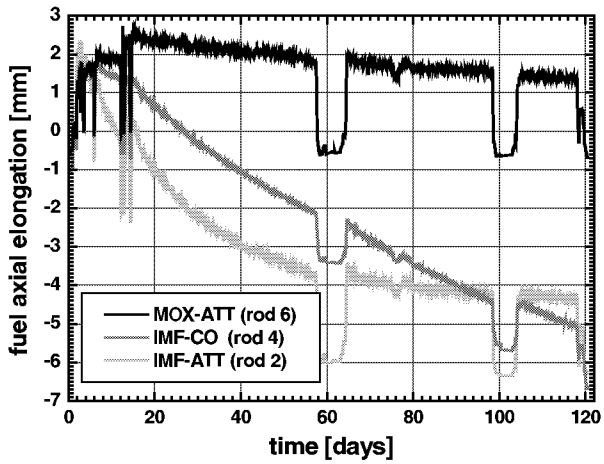

Fig. 7: Fuel axial elongation vs. time in IFA-651.1.

3.2 Fuel Modelling

For the instrumentation of the fuel pins, and the estimation of the fuel behaviour in order to fix safety limits, calculations had to be performed prior to irradiation. This was done with a modified version of the code TRANSURANUS (V1M1J99) [15]. The TRANSURANUS code turned out to be very suitable for this purpose as it allows the implementation of a wide range of new models into the mathematically stable framework of the code. As only very few data for IMF, i.e. (Er,Y,Pu,Zr)O_{2-x}, are available, large uncertainties must be attached to the prediction of the fuel centre temperature and fission gas release. Nevertheless, modelling was useful in support of the layout of the experiment, and to identify crucial parameters for fuel behaviour.

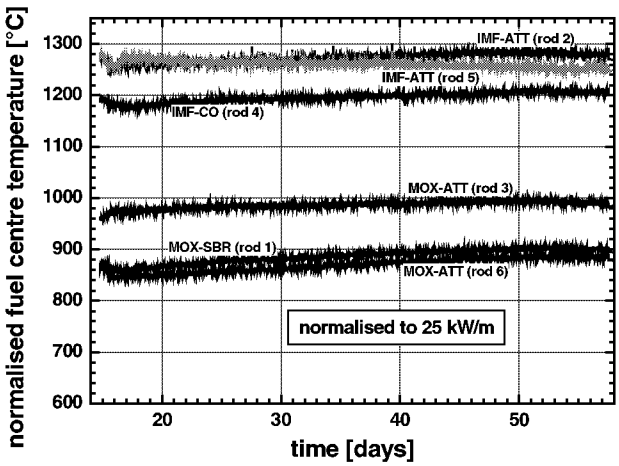

Fig. 8: Normalised temperatures vs. time for IFA-651.1.

Modification of the code was done by adapting data to suit IMF or related material. For IMF, a thermal conductivity of 1.9 W/(K*m) for all temperatures was used [16]. The radial power distribution was taken from a HELIOS calculation, and used as table-input in TRANSURANUS. The actual and theoretical density of IMF was measured during the fabrication. No other correlations or models are known for IMF. As YSZ is widely used for engineering purposes, thermal expansion at room temperature, yield stress, Young's modulus, emissivity, melting temperature and specific heat are are all well known, and were consequently used for modelling IMF. In the case of unknown IMF or YSZ material correlations, the standard correlations for UO_2 were used (swelling, creep strain), according to irradiation tests for ZrO_2-UO_2 [17,18]. The TRANSURANUS standard fission gas release model for UO_2 was used as a first approximation with regard to diffusion experiments with Cs and I in single-phase $(Y,Ce,Zr)O_2$ [19,20]. The modified code allowed a fast adaptation of the different models to the observed behaviour of IMF.

The densification model, and either the thermal conductivity or the relocation model, had to be modified after the data from the first cycle became available. As, up to now, no fission gas release could be observed (due to the relatively low burn-up), the fission gas release model could not be tested or modified.

Densification was first modelled with a simple densification model. This model, which gives reasonable results for MOX, could not reproduce the data obtained during the first 120 days of irradiation. As IMF shows strong densification, but nearly no increase in fuel centre temperature (which would reveal a homogeneous sintering with an increase of the gap), the gap size must stay nearly unaffected by the densification process.

A new model is proposed which takes into account the experimental results. The model assumes an immediate fragmentation of the fuel due to thermal stresses, which causes also relocation. The fragments of the fuel are placed in a strong temperature gradient due to the low thermal conductivity of IMF. Densification starts in the hot centre zone of the cracked fuel pellets. The single pieces of fuel are restricted in their relative movement by the colder outer fuel zones. Therefore, the hot centre edges of the fragments (which are of pie-slice shape) densify, and material is moved towards the colder fuel in the outer area. As irradiation proceeds, this process continues. Figure 9 shows a sketch of the proposed densification, which must always be regarded as isotropic: this means, when densification takes place, shrinkage of the fuel stack length must be modelled.

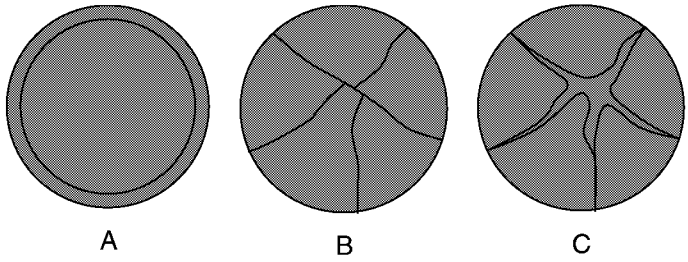

Fig. 9: Sketch of the proposed densification model.
A: fresh and densified pellet due to the MOX-densification model.
B: fresh pellet with cracks due to the IMF-densification model.
C: densified pellet with increased open crack volume due to the IMF-densification model.

Four additional comments must be given regarding this model. Firstly, the model can be definitely confirmed only after PIE (by neutronradiography or micrographs). Secondly, the fuel centre temperatures are only measured in annular pellets: the model assumes no difference between annular and solid pellets with regard to densification behaviour. Thirdly, the assumed cracks are parallel to the direction of the heat transport, and do not reduce the thermal conductivity. On the contrary, the thermal conductivity is increased by the loss of porosity due to densification. Fourthly, this model describes an extreme view of the mechanisms. In reality, a certain growth in gap size might be observed. This is taken into account by a factor defining the weighting between the simple densification model and the proposed new model.

The new model was implemented in TRANSURANUS using the "crack volume". This volume was defined to keep the mass constant while the diameter of the pellet increases due to relocation. The crack volume does not influence the thermal conductivity by the porosity correction in the new model. The lateral amount of the free volume gained by densification is added to the crack volume, while the axial amount of the densification is used to model a decrease in fuel stack length. In order to keep the implemented model simple, no temperature dependence is used in the implementation. Therefore, the processes in the hot

fuel centre zone (where sintering is immediately noticed by the PFs), and in the colder outer fuel region (where the ETs detect sintering), are taking place virtually at the same time. In fact, the experimental results show, in accordance with the proposed model, that the ETs detect slightly slower sintering than the PFs.

Results of the TRANSURANUS modelling are compared with the experimental results for rod 2 in Fig. 10 to Fig. 12. The inner pin pressure and the fuel stack length could be modelled satisfactorily well. The qualitative similarity of the fuel elongation data is very good. The quantitative difference in fuel stack length cannot be explained by axial relocation, nor by different thermal expansion, but is most probably due to experimental effects.

The temperatures do not only depend on the thermal conductivity and the densification model, but also on the relocation model. Relocation means the decreasing of the gap by a slight relocation of the pellet segments towards the cladding. Modelling the experiment without a relocation model would lead to differences between measurement and calculation of 20 to 30°C at maximum, which could be regarded as a very good agreement. But, since experience with ceramic fuel and the proposed densification model both indicate that relocation takes place, a relocation model should be applied in the calculation.

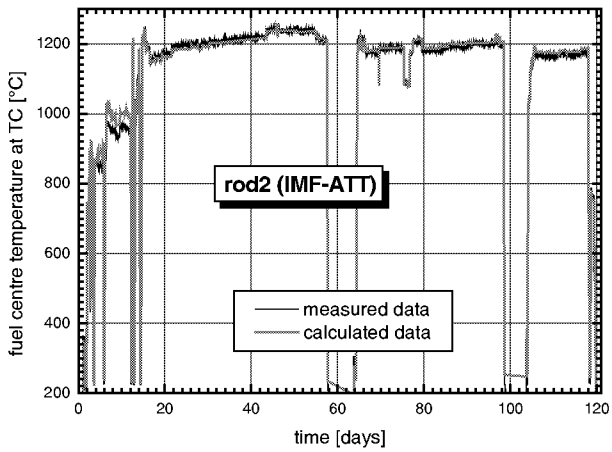

Fig. 10: Measured and calculated temperatures for rod 2 (IMF-ATT).

The relocation of the fuel is caused by thermal stresses, and depends on the temperature distribution, the thermal expansion, the Young's modulus, and the yield strength of the fuel. The UO_2 relocation model of the GAPCON-3 code was used in TRANSURANUS to model the MOX fuel, and achieved reasonable results. When this model is used for the IMF rod, the thermal conductivity of IMF must be reduced from 1.9 to 1.75 W/(K*m) to give agreement between experiment and calculation within 30°C. If the thermal conductivity is left untouched, the relocation model might be adjusted to the experimental results.

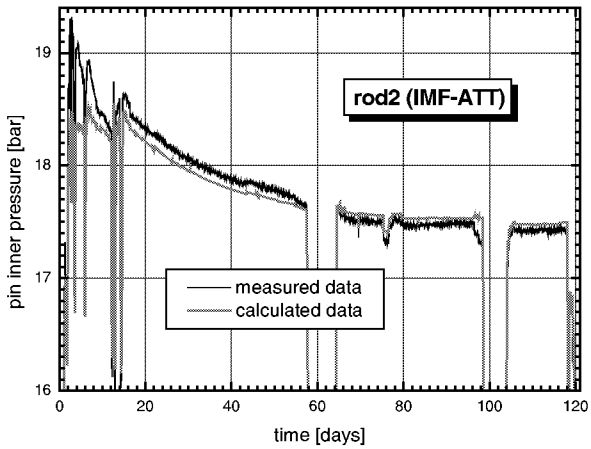

Fig. 11: Measured and calculated pin inner pressures for rod 2 (IMF-ATT).

The results shown in Fig.10 to Fig.12 have been calculated using the previously given thermal conductivity of 1.9 W/(K*m), and a modified GAPCON-3 relocation model. The modification consisted of limiting the (relocation-driving) linear heat rate to 18 kW/m, and adding a factor 0.5 to the relocation strain. Although some evidence for this procedure was found in the experimental data, it must be clearly pointed out that there is no theoretical or larger experimental basis for the assumption. To conclude, modifications to thermal conductivity and relocation are interchangeable to a certain extent, giving satisfactory agreement between experiment and calculation (without affecting significantly the pin pressure or the fuel stack elongation results). No further conclusions can be drawn from the available data.

In the second cycle, the power will be enhanced to over 32 kW/m. The temperatures, which will then be reached in IMF, would cause fission gas release (FGR) in MOX fuel, and will be predicted by TRANSURANUS using the UO_2 FGR model. At temperatures above 1400°C, the potential for fission gas retention in IMF not only depends on the retention potential of the matrix, but also on the stability of the grain boundaries. Grain boundary movement during restructuring and pore migration would sweep the fission gas to the grain boundaries, and shorten the release path. While no significant pore migration is expected in the second cycle for IMF-ATT (the material reached 100%TD during the first cycle), IMF-CO might show this effect. Restructuring could take place in the IMF rods during the second cycle, and might trigger FGR. Differences between IMF-ATT and IMF-CO can also be expected for these processes due to the different as-fabricated grain structure.

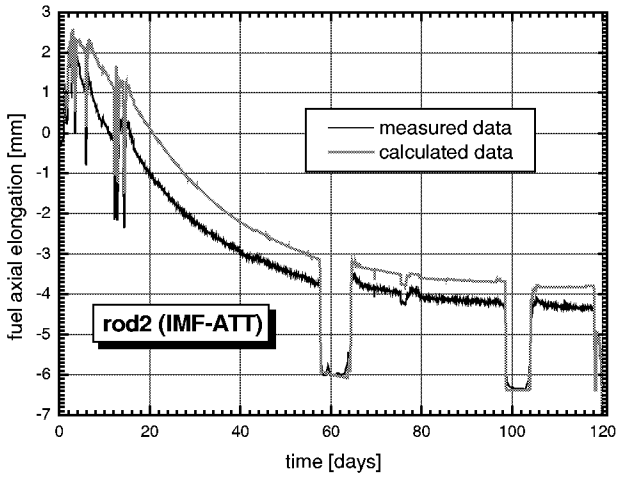

Fig. 12: Measured and calculated fuel stack lengths for rod 2 (IMF-ATT).

4 CONCLUSIONS

The IMF/MOX irradiation test in Halden has started successfully and a large amount of valuable data has been collected. The neutronic behaviour could be predicted accurately, and the fuel temperatures are within the expected range. The measured temperatures can be modelled well using a modified relocation model. The proposed thermal conductivity of IMF could not be validated due to the dependence of the fuel temperatures on the unknown relocation behaviour. The unexpectedly strong densification, which occurred during the first irradiation cycle, does not alter the fuel temperatures. A new densification model with an increase of the open crack volume is proposed to explain the experimental findings. The high densification might be of advantage for fission gas retention when higher linear heat rates are reached during the second cycle, because no pore migration would then sweep out the gas. In general, the FGR will be the main area of interest during the second cycle.

ACKNOWLEDGMENTS

The work of G. Ledergerber and C. Degueldre on IMF was fundamental for this project at PSI. The fabrication and irradiation became possible by the collaboration with KAERI (D.S. Sohn, Y.-W. Lee, H.S. Kim), BNFL (Ch. Brown, G.A. Gates), and the OECD Halden Project (W. Wiesenack, G. Rossiter, B.H. Lee). The fuel fabrication at PSI was directed by P. Heimgartner. The authors would also like to thank the Swiss utilities for the financial support given to the actinide and fuel research work at PSI.

REFERENCES

[1] C. Degueldre, U. Kasemeyer, F. Botta, G. Ledergerber, *"Plutonium incineration in LWR's by a once-through cycle with a rock-like fuel"*, Material Research Society Symposium Proceedings, **412**, 15-23 (1995).

[2] U. Kasemeyer, P. Grimm, J.M. Paratte, R. Chawla, *"Comparison of PWR Core Characteristics for 100% Pu-containing Loadings"*, Nuclear Technology, **122**, 52-63 (1998).

[3] E. Curti, W. Hummel, *"Modelling the solubility of zirconia in a repository for high-level radioactive waste"*, Journal of Nuclear Materials, **274,** 189-196 (1999).

[4] U. Kasemeyer, *"Konzeption eines uranfreien LWR-Kerns zur Plutoniumverbrennung"*, PhD Thesis, EPFL Lausanne, Switzerland (1998).

[5] M.A. Pouchon, *"Contribution to the study of a zirconia based nuclear fuel for plutonium use in light water reactor"*, PhD Thesis, University of Geneva, Switzerland (1999).

[6] Y.-W. Lee, H.S. Kim, S.H. Kim, C.Y. Joung, S.C. Lee, S.H. Na, P. Heimgartner, G. Ledergerber, *"Study on the basic mechanical property and behavior against thermal shock of simulated ZrO2-based inert matrix fuel material"*, Proc. of the EMRS Symposium B, 30 May-2 June, Strasbourg, France (2000).

[7] M. Burghartz, G. Ledergerber, F. Ingold, P. Heimgartner, C. Degueldre, *"X-ray diffraction analysis and data interpretation of stabilised zirconia doped with plutonium"*, Proc. of the EMRS Symposium B, 30 May-2 June, Strasbourg, France (2000).

[8] C. Degueldre, M.A. Pouchon, M. Streit, O. Zaharko, *"Analysis of porous features of zirconia based inert matrix and impact on the material qualification"*, Proc. of the EMRS Symposium B, 30 May-2 June, Strasbourg, France (2000).

[9] M.A. Pouchon, M. Döbeli, C. Degueldre, *"Thermal stability of implanted fission product elements in yttria stabilised zirconia"*, Proc. of the EMRS Symposium B, 30 May-2 June, Strasbourg, France (2000).

[10] U. Kasemeyer, Y.-W. Lee, G. Ledergerber, D.S. Sohn, G.A. Gates, Ch. Hellwig, W. Wiesenack, *"The irradiation of inert matrix fuel in comparison to MOX in the Halden reactor"*, Proc. of the EMRS Symposium B, 30 May-2 June, Strasbourg, France (2000).

[11] R.J.J. Stammler (Ed.), *"HELIOS Documentation"*, FMS, the Scandpower Fuel Management System (1995).

[12] C.L. Dunford, *"Evaluated Nuclear Data File, ENDF/B-VI"*, Proc. of Inter. Conf. on Nuclear Data for Science and Technology, Jülich (1991).

[13] Y.-W. Lee, G. Ledergerber, H.S. Kim, P. Heimgartner, S.H. Kim, C.Y. Joung, S.H. Na, M. Pouchon, M. Burghartz, *"Preparation of Simulated Inert Matrix Fuel with Different Powders by Dry Milling Method"*, Journal of Nuclear Materials, **274**, 7-14 (1999).

[14] Ch. Brown, P. Cook, J. Edwards, S. Fisher, G. Gates, I. Palmer, R. White, *"Performance of BNFL SBR MOX Fuel for the Next Decade"*, TOPFUEL99, 223 (1999).

[15] K. Lassmann, J. van de Laar, *„TRANSURANUS Handbook, Version 1 Modification 2 Year 1998"*, European Commission, Joint Research Centre, Inst. f. Transuranium Elements, Karlsruhe, Germany (1998).

[16] M.A. Pouchon, C. Degueldre, P. Tissot, *"Determination of the thermal conductivity in zirconia based inert matrix nuclear fuel by oscillating differential scanning calorimetry and laser flash"*, Thermochimica Acta, **323**, 109-121 (1998).

[17] B.F. Rubin, R.M. Berman und M.L. Bleiberg, "*The irradiation behaviour of ZrO_2-UO_2 fuels"*, WAPD-264, UC-25: Metals, Ceramics, and Materials (TID-4500 (17^{th} Edition), Bettis Atomic Power Lab., Pittsburgh, PA., USA (1962).

[18] M.D. Freshley und D.F. Carroll, *"The irradiation performance of ZrO_2-PuO_2 nuclear fuel"*, American Society Winter Meeting, November 17-21, New York City, New York, USA (1963).

[19] M.A. Pouchon, M. Döbeli, C. Degueldre, *"Retention of iodine in yttria stabilised zirconia"*, Nuclear Instruments and Methods in Physics Research Section B, **148**, 783-786 (1999).

[20] M.A. Pouchon, M. Döbeli, C. Degueldre, M. Burghartz, *"Behavior of cesium implanted in zirconia based inert matrix fuel"*, Journal of Nuclear Materials, **274**, 61-65 (1999).